Lab on a Chip

PAPER

Early development drug formulation on a chip: Fabrication of nanoparticles using a microfluidic spray dryer†

Julian Thiele,[ab] Maike Windbergs,[a] Adam R. Abate,[a] Martin Trebbin,[b] Ho Cheung Shum,[‡a] Stephan Förster[b] and David A. Weitz[*a]

Early development drug formulation is exacerbated by increasingly poor bioavailability of potential candidates. Prevention of attrition due to formulation problems necessitates physicochemical analysis and formulation studies at a very early stage during development, where the availability of a new substance is limited to small quantities, thus impeding extensive experiments. Miniaturization of common formulation processes is a strategy to overcome those limitations. We present a versatile technique for fabricating drug nanoformulations using a microfluidic spray dryer. Nanoparticles are formed by evaporative precipitation of the drug-loaded spray in air at room temperature. Using danazol as a model drug, amorphous nanoparticles of 20–60 nm in diameter are prepared with a narrow size distribution. We design the device with a geometry that allows the injection of two separate solvent streams, thus enabling co-spray drying of two substances for the production of drug co-precipitates with tailor-made composition for optimization of therapeutic efficiency.

Introduction

The development of novel pharmaceuticals is a challenging field involving cost-intensive research in combination with a high attrition rate of potential candidates.[1,2] Due to high-throughput technologies an increasing number of new chemical entities with potential therapeutic efficiency is identified.[3,4] Unfortunately, the molecular complexity of drugs has significantly increased over the last decade.[5–7] Although molecular complexity usually contributes to biological activity, it often causes poor solubility of drugs.[6,8] This limits their bioavailability in the human body, and the reason for attrition of pharmacologically promising substances can often be found in the failure to develop a suitable formulation for therapeutic application.[9] Prevention of failure due to formulation limitations necessitates physicochemical analysis and formulation studies at a very early stage during development.[10,11] At this stage, the availability of the drug candidate is limited to small amounts, thus hampering extensive experiments.

One suitable approach to increase the bioavailability of a drug is to reduce the particle size, which increases the specific surface and, therefore, facilitates release and absorption of the drug.[12–15] Furthermore, increased bioavailability can be achieved by amorphization of the sample. In this context, spray drying is a powerful technique enabling instantaneous drying of solutions, emulsions or suspensions in one step. The final product is a fine, often amorphous powder with a large surface. Pharmaceutical application of spray drying techniques are ubiquitous; their use ranges from the manufacture of dry plant extracts for avoiding decomposition of thermally degradable components, to the production of excipients for compression with improved binding characteristics.[16–18] Furthermore, the technique is successfully used for co-precipitation of a drug and another substance to increase the drug's bioavailability.[19] However unfortunately, in case of early stage formulation development the use of conventional spray drying setups is restricted. Conventional spray drying equipment requires large amounts of sample as the dead volume of the apparatus is rather large and a considerable portion of discard material is generated during the process. Furthermore, the optimization of processing parameters necessitates additional quantities of sample to receive a homogeneous product. Moreover, particle sizes below 100 nm, as often required for targeted drug delivery, are extremely hard to generate.[20,21] An appropriate application for spray drying for early development drug formulation would require the miniaturization of the setup. These limitations can be overcome using microfluidic techniques.[22–26] Extremely small volumes can precisely be handled on microfluidic chips enabling the controlled generation of homogeneous products as well as a fast change of process conditions. It would be highly desirable to

[a]School of Engineering and Applied Sciences, Department of Physics, Harvard University, Cambridge, Massachusetts, USA. E-mail: weitz@seas.harvard.edu; Fax: +617-495-3275; Tel: +617-495-3275
[b]Physical Chemistry I, University of Bayreuth, Germany
† Electronic supplementary information (ESI) available. See DOI: 10.1039/c1lc20298g
‡ Current address: Department of Mechanical Engineering, University of Hong Kong, Hong Kong

design a microfluidic chip which combines the versatility of microfluidics with the ability to formulate drug particles with high accuracy using spray drying techniques.

In this paper, we present the first microfluidic spray dryer on a poly(dimethylsiloxane) (PDMS) chip.[27–29] We use the hydrophobic model drug danazol to test the new device. By controlling the collection distance of the spray, we can control the crystallinity of the product. Our microfluidic device enables fabrication of drug nanoparticles with sizes of less than 100 nm in diameter. The versatile device design also enables the formation of amorphous co-precipitates by co-spray drying two substances.

Results and discussion

In conventional spray dryers, a single liquid stream is typically vaporized by compressed air in a spray nozzle; the spray is then mixed with a heated gas stream in a drying chamber to evaporate the solvent and yield the dry product.[21] However, this setup only allows processing of single solvent systems or mixtures of pre-mixed solvents. To process multiple separate solvent streams as required for solvent/antisolvent precipitation or rapidly reacting solvent streams, the spray dryer generally needs to be equipped with additional separate inlet channels.[30] In this work, we use a microfluidic device with an array of two flow-focusing cross junctions, as shown in Fig. 1.

The device enables separate injection of two solvents and provides a third inlet for compressed air to form the spray. For the formation of hydrophobic drug nanoparticles, we dissolve the hydrophobic drug danazol in an organic solvent injected into the first inlet, and inject the second fluid into the second inlet. The two solvents form a jet at the first cross junction, which extends into the second cross junction where compressed air is injected to form the spray. To process hydrophobic drugs, the PDMS device must resist fouling due to adsorption of drug crystals on the microchannel walls.[31,32] This is especially crucial when starting up the device, as potential backflow of the drug-loaded solvent stream into the anti-solvent reservoir, and *vice versa*, can cause significant precipitation of the hydrophobic drug in the microchannels. To prevent adsorption of the drug on the microchannel walls, we treat the intrinsically hydrophobic PDMS device with oxygen plasma, as the plasma renders the walls of the device hydrophilic.[33] Although the hydrophilicity of the plasma treated device decreases over time,
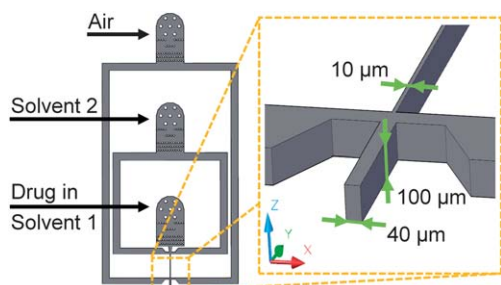
the channel surface can easily be regenerated in the same manner multiple times. However, for early development drug formulation, the amount of sample is extremely small thus being the limiting factor in such an experiment rather than the duration of a surface plasma treatment. In addition, we minimize the surface contact between the drug-loaded solvent stream and the channel walls. We achieve this by designing a device geometry with a high aspect ratio. The ratio h/w is 10 : 1 in the upper half of the device and 4 : 1 at the spray nozzle. Although high-aspect-ratio channel geometries are generally known to increase surface interactions,[34] microchannels with a high aspect ratio are less pressure-resistant than squared channels, when fabricated in the rather soft PDMS;
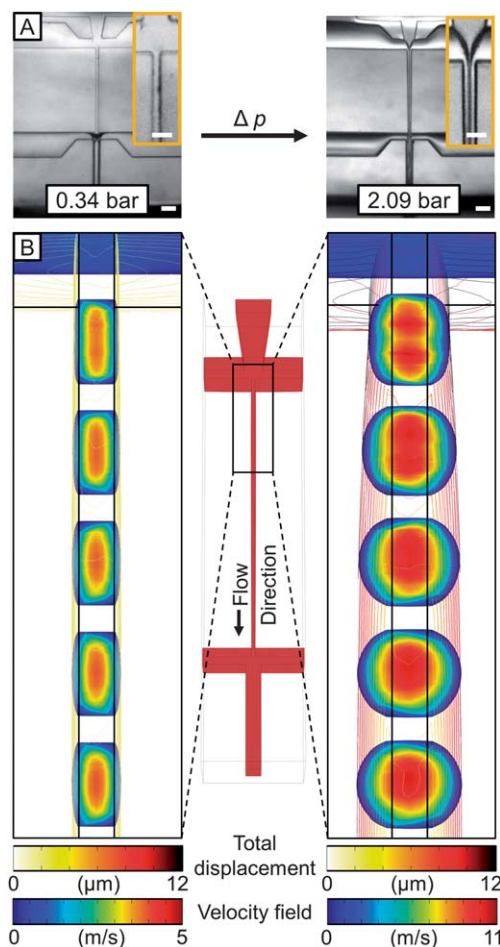

Fig. 2 Pressure-induced deformation of the microfluidic spray dryer during operation. (A) Bright-field microscopy images of the microfluidic spray dryer at low pressure (left) and operating pressure (right). The dark fields in the microchannels indicate the curvature of the channel walls causing the light to scatter. The scale bars denote 50 μm, scale bars for the magnified view are 20 μm. (B) The impact of the deformation on the flow profile is studied using CFD simulations based on the finite element method. The initial rectangular microchannels (left) expand and adopt a circular shape (right). This deformation changes the flow pattern from a two dimensional focused flow to an elliptic to coaxial flow, therefore reducing the contact between the drug-loaded solvent stream and the channels walls. To emphasize the deformation, the simulation model is viewed from an angle of approximately 30° above the second cross junction, and the original position of the microchannel walls is added as black lines to the simulation model.

Fig. 1 Schematic of a microfluidic device for forming nanoparticles from hydrophobic drugs by spray drying. The microfluidic device is rendered hydrophilic with an oxygen plasma treatment. The device geometry enables separate injection of two solvent streams of which the spray is formed.

thus the operating spray dryer channels easily expand, as shown in Fig. 2.

To determine the impact of the channel deformation on the flow profile, we process a typical solvent/antisolvent system in our spray dryer and compare the device deformation at low and high flow rates and air pressure, respectively. Our observations are supported by computational fluid dynamics (CFD) simulations coupled with fluid-structure interaction (FSI) using COMSOL 4.1.0.185. We design a 3D simulation model of the microfluidic spray dryer considering the solid mechanics of the device described by a linear elastic model and the fluid flow therein described by the Navier–Stokes equations. For the device building material PDMS, which is mixed from the pre-polymer and crosslinker in a ratio of 10 : 1, Young's modulus is approximately 4 MPa, the Poisson's Ratio is 0.42, and the density is 920 kg m^{-3}.[35,36] The model consists of 62 713 finite elements with an average mesh quality of 0.8003 on a scale of 0 to 1, where 1 is the highest quality. The model is solved for 401 878 degrees of freedom. A detailed discussion of the simulation model and its mathematical background is provided in the ESI† for this publication. For the spray experiment at low flow rates and low pressure, we inject isopropyl alcohol (IPA) as the solvent, water as the anti-solvent and compressed air into the first, second and third inlet, respectively, at flow rates of 1 mL h^{-1} for the inner phase and 10 mL h^{-1} for the middle phase. The air pressure is set to 0.34 bar. For the high-flow rate/high-pressure experiment, we increase the flow rates of IPA and water to 5 mL h^{-1} and 50 mL h^{-1}, respectively, and set the air pressure to 2.09 bar. At low pressure (0.34 bar), the PDMS device demonstrates minimal deformation and we observe a two dimensional focused flow pattern between the first and second cross junction. However, as we increase the pressure, the PDMS device responds to the internal stress and expands, as shown in the magnified view of Fig. 2A. Due to the high aspect ratio, the largest expansion of the microchannels is observed in the side walls of the channels. Image analysis of microscope images shows that the microchannels widen by an average factor of two, as shown in the magnified views in Fig. 2A. This deformation strongly influences the flow profile inside the spray dryer, as shown in the corresponding simulations in Fig. 2B. As illustrated by the slice plot of the simulated velocity profile, the flow between the first and second cross junction adopts a three dimensional flow pattern, similar to that observed in microfluidic capillary devices.[37] Thereby, the inner phase is surrounded by a protective sheath of the middle phase, as shown in the magnified view of Fig. 2A (right). This minimizes the surface contact of the solvent in which the hydrophobic drug is dissolved with the channel walls and prevents fouling of our device.

When forming a spray, the spray shape and drop size are important factors influencing drying, particle size and morphology of the processed drug. To determine drop size and spray shape, we visualize the spray formation in our spray dryer with a high-speed camera. We inject IPA into the first and second inlet at a total flow rate of 55 mL h^{-1}. At low air pressure, the solvent stream is not dispersed into a spray; instead, a jet of liquid is ejected from the spray nozzle and breaks into large droplets due to Rayleigh-Plateau instability, as shown in Fig. 3A.[37] As the air pressure is increased beyond 0.5 bar, we observe the formation of a mixture of large drops and finely
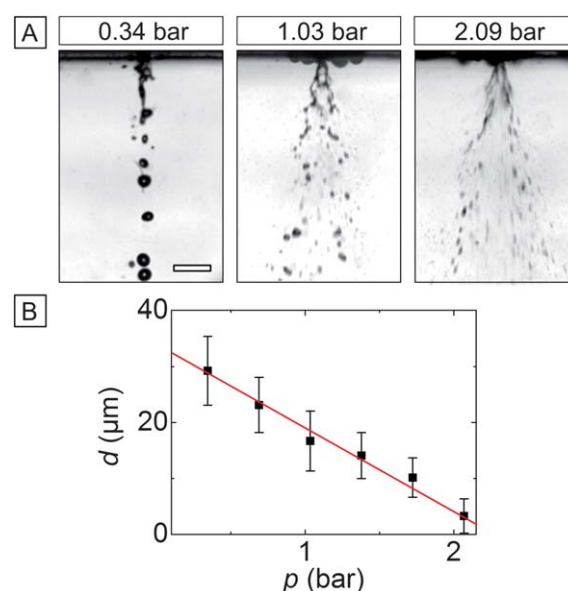
Fig. 3 (A) Spray profile of the nozzle for different air pressures. IPA is injected into the spray dryer at 55 mL h^{-1}. At low pressure, a fluid jet is ejected from the nozzle which breaks into single droplets downstream. When the pressure is increased beyond 0.5 bar, the spray profile adopts a cone-like shape. The scale bar for all panels denotes 100 μm. (B) Drop diameter as a function of p. With increasing pressure, the mean size of the droplets decreases linearly. At a pressure of 2.09 bar, the droplets are approximately 4 μm in diameter. The red line is a guide to the eye.

dispersed drops at the spray nozzle; the onset of spraying can be confirmed by the round full cone pattern adopted by the droplets formed, that appears as a triangular spray pattern in the side view of the high-speed camera. This precise pattern is formed due to turbulences imparted to the liquid prior to the orifice in the short outlet channel. To quantify the spray formation process, we measure the drop size d as a function of the air pressure p, as shown in Fig. 3B. The drop size decreases linearly with increasing pressure to approximately 4 μm in diameter at 2.1 bar, which is the maximum pressure our spray dryer can withstand without delamination of the plasma-bonded PDMS.

We demonstrate the concept to form hydrophobic drug nanoparticles with our microfluidic spray dryer. Danazol is used as a model drug, which is an isoxazole derivative of testosterone and applied for the treatment of endometriosis and hereditary angioedema.[23] In general, a convenient method for processing hydrophobic drugs is liquid antisolvent precipitation (LASP), where the drug, dissolved in an alcohol, is precipitated by mixing the drug solution with water as the antisolvent.[16,38] We dissolve danazol in isopropyl alcohol and inject it together with water into the first cross junction. As we operate our microfluidic device in the laminar flow regime, only diffusion based mixing of the solvent streams is observed at their interfaces. To evaluate the effect of microfluidic processing alone on the particle size and morphology of the hydrophobic drug, no stabilizer or surfactant is added to influence the particle growth, nor do we use common co-solvents such as DMSO and benzyl alcohol. We set the flow rates to 5 mL h^{-1} for danazol, and 50 mL h^{-1} for water, which corresponds to a volumetric ratio of 1 : 10 and has been shown to yield danazol microparticles in conventional LASP processes.[23]

The spray is suspended in air, thus ensuring that the product is dried upon collection. We examine the morphology and particle size of the processed drug using scanning electron microscopy (SEM). While unprocessed danazol is composed of particles with irregular shapes ranging from approximately 2 μm to 100 μm, the particle size is reduced significantly by processing the drug using our microfluidic spray dryer. As shown in Fig. 4A, we yield danazol nanoparticles with a narrow particle size distribution (PSD) from 20 nm to 60 nm and, therefore, smaller than previously reported.[7,23]

The formation of drug nanoparticles using LASP is driven by mixing of the drug solution with the antisolvent. Thus, the degree of supersaturation of the drug solution governs nucleation and growth of the drug nanoparticles.[16] However, sufficient mixing only occurs in the short outlet channel prior to the orifice of the spray nozzle in our microfluidic device. Since we use high flow rates to form a stable spray, the delay time of the fluids in the outlet channel should be too short to enable growth of the drug nuclei by mixing. To reveal the formation process, we replace the antisolvent with the solvent, and inject a solution of danazol in IPA and pure IPA into the first and second inlet, respectively. The formation of danazol nanoparticles of identical size and morphology in the absence of the antisolvent indicates that the particle formation is primarily driven by the evaporation of the spray and not by the formation of nuclei due to supersaturation, as shown in Fig. 4B. Our hypothesis is further supported by using a microfluidic spray dryer with a longer channel between the first and second nozzle and thus increased time of diffusion, which does not have a significant influence on the particle properties.

Another crucial aspect of the spray drying process is the distance from the spray drying nozzle at which the final product is collected. While it is known that the morphology and size of hydrophobic drugs depends on the initial concentration of reactants, the choice of additives and the ratio of solvent and antisolvent,[39] we find a significant dependence on the collection distance by performing spatial sampling of the spray. To illustrate this, we inject danazol and IPA as described above, but this time we collect the spray in steps of 5 cm from the spray nozzle. From our SEM analysis, two distinct product morphologies are revealed. At a collection distance of 5 cm, we observe an assembly of stacks of danazol; the thickness of each stack is about 60–80 nm, as shown in Fig. 5A. These values are in good agreement with the size of single danazol nanoparticles, as shown in Fig. 4A and 4B.

However, as the time of flight is too short to allow for complete evaporation of the spray upon collection, the remaining solvent increases the mobility of danazol particles on the collection substrate, allowing them to fuse and reach an energetically more favorable state.[16] We therefore increase the collection distance to 30 cm; as the spray is completely evaporated, single nanoparticles are formed, that become densely packed over the long time of sample collection, as shown in Fig. 5B. X-ray powder diffraction analysis (XRD) is employed to determine the effect of spatial sampling on the crystallinity of danazol. We use the characteristic peaks at 2θ of 15.8, 17.1 and 19.0 in the XRD pattern of unprocessed danazol as a reference. In processed danazol, the intensity of the characteristic peaks decreases as the collection distance of the spray is increased. This indicates that the initial crystallinity of the drug is not recovered, as shown in Fig. 5C. The formation of amorphous danazol is of importance, as the difference in physicochemical properties of the amorphous form significantly increases the bioavailability of danazol.[23]

Another way to fabricate amorphous hydrophobic drug particles is to co-spray dry the drug and a crystallization inhibitor.[40] As a control experiment, we first co-spray dry danazol in IPA together with water and collect the spray at low distance. As shown before, the spray is not completely evaporated due to the short time of flight. This allows danazol to grow into star-shape crystalline aggregates, as shown in Fig. 6A. We use poly(vinyl-pyrrolidone) (PVP) as a substance for co-spray drying with
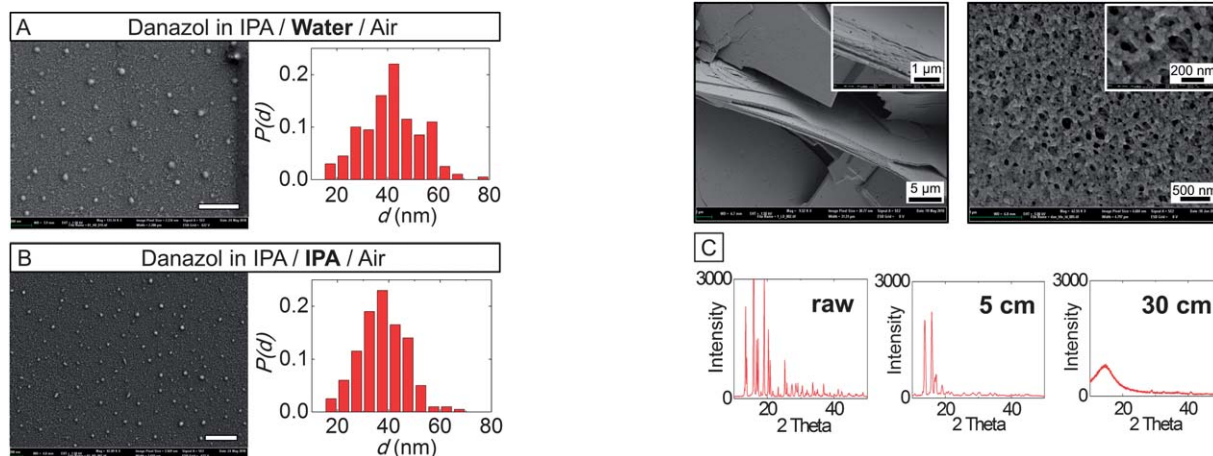
Fig. 4 Effect of the solvent system on particle size and composition. Danazol in IPA is mixed with (A) water as the antisolvent, or (B) IPA as the solvent inside the microfluidic spray dryer. In either case, nanoparticles are produced with a narrow PSD and an average diameter of 20–60 nm. Scale bars denote 300 nm.

Fig. 5 Spatial sampling of processed danazol. Depending on the collection distance, various morphologies are observed; (A) assembly of stacks with a thickness of 60–80 nm, and (B) nanoparticles, approximately 20 nm to 60 nm in diameter, assembled in a dense network. (C) XRD patterns of processed danazol collected at a distance of 5 cm and 30 cm from the spray nozzle, and unprocessed danazol as a reference.
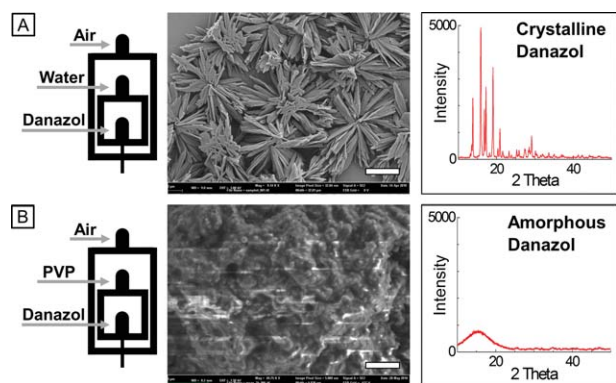
Fig. 6 Inhibition of danazol crystallization by PVP. (A) Danazol in IPA is mixed with water inside the microfluidic device; the spray is collected at a distance of 1 cm from the nozzle, allowing danazol to grow into crystalline aggregates, as indicated by the XRD pattern. The scale bar is 5 μm. (B) By processing danazol in IPA and an aqueous solution of PVP, which are injected separately into our spray dryer, amorphous co-precipitates are yielded, as indicated by the corresponding XRD pattern. The scale bar denotes 500 nm.

Fig. 7 Fabrication of danazol particles and danazol/PVP co-precipitates in a conventional spray dryer using the same formulations as in our microfluidic device. (A) Instead of amorphous drug nanoparticles, crystalline particles, and (B) microscopic co-precipitates are yielded.

danazol to fabricate amorphous co-precipitates, as PVP is known to inhibit crystal growth in pharmaceutical formulations.[41–44] We process danazol in IPA together with a 1.5 wt% solution of PVP in water at equal flow rates of 25 mL h^{-1}. Again, the spray is collected at short distance. However, as the spray is dried, danazol precipitates from the spray in a combination with PVP without crystallization, thus no characteristic peaks are observed in the XRD pattern, as shown in Fig. 6B.

To relate the performance of our microfluidic spray dryer to conventional spray dryers, we perform spray drying experiments with the same formulations and compare the results by XRD and SEM. We use the well-established and widely known Mini Spray Dryer B-191 (Buechi, Germany) with a spray rate of 10 mg min^{-1}, and process a solution of danazol in IPA without and with PVP, respectively. In both cases, we yield particles ranging from approximately 1 μm to 5 μm, which are substantially larger than the danazol particles formed with our microfluidic spray dryer. Moreover, the degree of crystallinity of the resultant danazol particles without PVP is high, as shown in Fig. 7A. We assume that the smaller drop and particle size using our microfluidic spray dryer is achieved due to the well-controllable flow conditions in the microfluidic device and the use of pulsation-free syringe pumps, which enable a degree of control over the spray formation and mixing prior to the nozzle that cannot be achieved in conventional macro-sized setups and eventually leads to the formation of particles below 100 nm, as we have observed in our studies.

However, the development of laboratory spray dryers towards benchmarking the minimal particle size is an ongoing process, though, and we expect novel equipment such as the Buechi B-90 to fabricate particles with submicron-size using our formulations. However, with the intended use for early drug formulation development, our spray drying approach exhibits several advantages, which cannot be realized in a common spray dryer. The dead volume of our chip is extremely small, thus avoiding waste of the sample and facilitating experiments with minimal sample volume. Furthermore, chip design and fabrication is easy
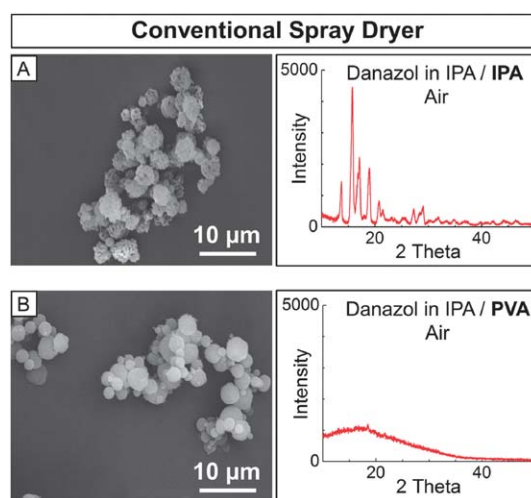
and extremely flexible in terms of geometry, thereby allowing customized design. As drugs in their early development stage lack a complete toxicological profile, handling and cleaning of contaminated equipment has to be performed with high safety precautions. As the fabrication of our chip is inexpensive and easy, it can just be discarded after use. An additional advantage of our chip is sample collection. Due to the flexible setup the particles can directly be collected in vials or on sample holders for further characterization, thus avoiding waste and alteration of sample properties.

Experimental

Device fabrication

The PDMS microfluidic devices are fabricated using soft lithography.[27] All channels have a fixed height of 100 μm. The PDMS replica is bonded to a flat sheet of cured PDMS using oxygen plasma treatment. The plasma treatment renders the microchannels temporarily hydrophilic.[33] To retain the hydrophilic surface modification, suitable for handling hydrophobic drugs, the device is flushed with deionized water. The nozzle of the spray dryer is prepared by slicing the outlet channel of the stamped device with a razor blade. To achieve reproducible accuracy when slicing, we include a guide to the eye in the initial AutoCAD design of the spray dryer.

Spray drying experiments

PVP (weight-averaged molecular weight, M_W 10 000 g mol^{-1}) and all other chemicals are obtained from Sigma-Aldrich Co. unless noted otherwise. Danazol (99.9%) is obtained from Selectchemie AG. Water with a resistivity of 16.8 MΩ cm^{-1} is prepared using a Millipore Milli-Q system. All solutions are filtered through a 0.2 μm PTFE filter (Millipore). We form danazol nanoparticles using our microfluidic spray dryer. To demonstrate long term stability of the process, each experiment is performed over a time period of 2 h. We inject a saturated

solution of danazol in IPA into the first inlet and water or IPA into the second inlet at 5 mL h⁻¹ and 50 mL h⁻¹, respectively. For the formation of co-precipitates, we inject PVP in water (1.5% w/w) at 50 mL h⁻¹ into the second inlet. We fill the PE tubing that connects the syringe pumps with the device with pure IPA to prevent precipitation of the drug in the event of back flow of the drug-loaded solvent stream into the second solvent reservoir, and *vice versa*. To form the spray, air is injected into the third inlet at 2.09 bar. The spray is ejected into air and dried at room temperature. We image the spray using a Phantom v9.1 camera (Vision Research) at 64 000 fps. The droplet size is obtained by measuring the size of at least 200 drops from high-speed camera images.

Product collection and characterization

Processed danazol is collected at distances between 5 cm and 30 cm from the spray nozzle. For SEM analysis, the spray is collected on glass slides and coated with Pd/Pt. We use an Ultra55 Field Emission SEM (Zeiss). The size distribution of the nanoparticles is determined by image analysis of SEM photographs using a public domain, Java-based image processing program, ImageJ. For XRD analysis and long-term experiments, samples are collected in an aluminum box over which the spray dryer is mounted. Due to the full-cone spray pattern, the dried product assembles in a circular pattern solely on the bottom of the collection box from which it is recovered in 70% to 95% yield. XRD analysis is performed using a Scintag XDS2000 powder diffractometer (Scintag, Cupertino, California, USA) with Cu-Kα radiation at 40 kV and 30 mA. The XRD patterns are taken at room temperature in the range of 10° ≤ 2θ ≤ 50° with a scan rate of 1° min⁻¹ and a step size of 0.02°.

Conclusions

Our microfluidic spray dryer is a versatile novel tool for early formulation development of new drug candidates. Precisely controlled generation of amorphous drug nanoparticles can successfully be realized requiring only small quantities of sample. The particles exhibit narrow size distribution and low mean particle sizes. By independent injection of two solvent streams, drug co-precipitates can be prepared as well. Our approach should also be useful for forming composite nanoparticles with freely tunable composition. As the spray is dried at room temperature, our microfluidic device also enables processing of thermally degradable materials. In addition, nanosuspensions, which can greatly enhance the dissolution rate and bioavailability of hydrophobic drugs, can be easily prepared by spraying the nanoparticles into a stabilizer solution. Therefore, our approach not only enables the formation of nanoprecipitates with a small particle size, but also improves the versatility of spray drying for manipulating the composition of the resultant nanoparticles. Design and fabrication of spray drying devices is easy and inexpensive, thereby allowing customized design for each formulation and disposal of the whole chip after use. As drug candidates during their early development phase lack a complete toxicological profile, this aspect is more than valuable contributing to safety and protection during development of new pharmaceuticals.

Notes and references

1 J. A. Masi, R. W. Hansen and H. G. Grabowski, *J. Health Econ.*, 2003, **22**, 151–185.
2 I. Kola and J. Landis, *Nat. Rev. Drug Discovery*, 2004, **3**, 711–715.
3 H. Kubinyi, *Nat. Rev. Drug Discovery*, 2003, **2**, 665–668.
4 X. Q. Chen, M. D. Autnan, C. Gesenberg and O. S. Gudmundsson, *AAPS PharmSciTech*, 2006, **8**, E402–208.
5 X. Chen, J. M. Vaughn, M. J. Yacaman, R. O. Williams III and K. P. Johnston, *J. Pharm. Sci.*, 2004, **93**, 1867–1878.
6 B. E. Rabinow, *Nat. Rev. Drug Discovery*, 2004, **3**, 785–796.
7 T. Panagiotou, S. V. Mesite and R. J. Fisher, *Ind. Eng. Chem. Res.*, 2009, **48**, 1761–1771.
8 A. Schuffenhauer, N. Brown, P. Selzer, P. Ertl and E. Jacoby, *J. Chem. Inf. Model.*, 2006, **46**, 525–535.
9 S. Venkatesh and R. A. Lipper, *J. Pharm. Sci.*, 2000, **89**, 145–154.
10 C. A. Lipinski, F. Lombardo, B. W. Dominy and P. J. Feeney, *Adv. Drug Delivery Rev.*, 1997, **23**, 3–25.
11 L. F. Huang and W. Q. Tony, *Adv. Drug Delivery Rev.*, 2004, **56**, 321–334.
12 P. Costa and J. M. S. Lobo, *Eur. J. Pharm. Sci.*, 2001, **13**, 123–133.
13 L. Gao, D. Zhang and M. Chen, *J. Nanopart. Res.*, 2008, **10**, 845–862.
14 E. Merisko-Liversidge, G. G. Liversidge and E. R. Cooper, *Eur. J. Pharm. Sci.*, 2003, **18**, 113–120.
15 F. Kesisoglou, S. Panmai and Y. Wu, *Adv. Drug Delivery Rev.*, 2007, **59**, 631–644.
16 R. Vehring, *Pharm. Res.*, 2008, **25**, 999–1022.
17 D. Chiou, T. A. G. Langrish and R. Braham, *J. Food Eng.*, 2008, **86**, 288–293.
18 Y. Gonnisson, S. I. Goncalves, J. P. Remon and C. Vervaet, *Drug Dev. Ind. Pharm.*, 2008, **34**, 248–257.
19 A. Paudel, J. Van Humbeeck and G. Van den Mooter, *Mol. Pharmaceutics*, 2010, **7**, 113–1148.
20 H. Gao, W. Shi and L. B. Freund, *Proc. Natl. Acad. Sci. U. S. A.*, 2005, **102**, 9469–9474.
21 X. Li, N. Anton, C. Arpagaus, F. Belleteix and T. F. Vandamme, *J. Controlled Release*, 2010, DOI: 10.1016/j.jconrel.2010.07.113.
22 H. S. M. Ali, P. York and N. Blagden, *Int. J. Pharm.*, 2009, **375**, 107–113.
23 H. Zhao, J.-X. Wang, Q.-A. Wang, J.-F. Chen and J. Yun, *Ind. Eng. Chem. Res.*, 2007, **46**, 8229–8235.
24 T. Tetradis-Meris, D. Rossetti, C. P. de Torres, R. Cao, G. Lian and R. Janes, *Ind. Eng. Chem. Res.*, 2009, **48**, 8881–8889.
25 P. W. Miller, L. E. Jennings, A. J. deMello, A. D. Gee, N. J. Long and R. Vilar, *Adv. Synth. Catal.*, 2009, **351**, 3260–3268.
26 A. S. Utada, E. Lorenceau, D. R. Link, P. D. Kaplan, H. A. Stone and D. A. Weitz, *Science*, 2005, **308**, 537–541.
27 Y. Xia and G. M. Whitesides, *Angew. Chem., Int. Ed.*, 1998, **37**, 550–575.
28 S. L. Peterson, A. McDonald, P. L. Gourley and D. Y. Sasaki, *Journal of Biomedical Materials Research Part A*, 2004, **72A**, 10–18.
29 D. B. Weibel and G. M. Whitesides, *Curr. Opin. Chem. Biol.*, 2006, **10**, 584–591.
30 T. Ozeki, S. Beppu, T. Mizoe, Y. Takashima, H. Yuasa and H. Okada, *Pharm. Res.*, 2006, **23**, 177–183.
31 P. Mayer, W. H. J. Vaes and J. L. M. Hermens, *Anal. Chem.*, 2000, **72**, 459–464.
32 M. Honest, H. K. Jin, L. Kwanseop, P. Nokyoung and H. H. Jong, *Electrophoresis*, 2003, **24**, 3607–3619.

33 B. Kim, E. T. K. Peterson, I. Papautsky, *Proceedings of the 26th Annual International Conference of the IEEE EMBS*, San Francisco, 2004, 5013–5016.
34 P. Mao and J. Han, *Lab Chip*, 2009, **9**, 586–591.
35 J. K. Deuschle, G. Buerki, H. M. Deuschle, S. Enders, J. Michler and E. Arzt, *Acta Mater.*, 2008, **56**, 4390–4401.
36 D. Armani, C. Liu, N. Aluru, *12th Int. Conf. IEEE MEMS*, 1999, 222–227.
37 A. S. Utada, L.-Y. Chu, A. Fernandez-Nieves, D. R. Link, C. Holtze and D. A. Weitz, *MRS Bull.*, 2007, **32**, 702–708.
38 J.-Y. Zhang, Z.-G. Shen, J. Zhong, T.-T. Hu, J.-F. Chen, Z.-Q. Ma and J. Yun, *Int. J. Pharm.*, 2006, **323**, 153–160.
39 S. D. Škapin and E. Matijević, *J. Colloid Interface Sci.*, 2004, **272**, 90–98.
40 S. M. Wong, I. W. Kellaway and S. Murdan, *Int. J. Pharm.*, 2006, **317**, 61–68.
41 H. Sekikawa, M. Nakano and T. Arita, *Chemical and Pharmaceutical Bulletin*, 1978, **26**, 118–126.
42 M. Yoshioka, B. C. Hancock and G. Zografi, *J. Pharm. Sci.*, 1995, **84**, 983–986.
43 L. S. Taylor and G. Zografi, *Pharm. Res.*, 1997, **14**, 1691–1698.
44 J.-H. Kim and H.-K. Choi, *International Journal of Pharmaceutics*, 2002, **236**, 81–85.